

# Critical exponents of the Ising model in three dimensions with long-range power-law correlated site disorder: A Monte Carlo study

 Stanislav Kazmin<sup>1,2,\*</sup> and Wolfhard Janke<sup>2</sup>
<sup>1</sup>Max Planck Institute for Mathematics in the Sciences, Inselstrasse 22, 04103 Leipzig, Germany

<sup>2</sup>Institut für Theoretische Physik, Universität Leipzig, IPF 231101, 04081 Leipzig, Germany


(Received 23 July 2021; revised 25 October 2021; accepted 27 April 2022; published 27 June 2022)

The critical behavior of the Ising model in three dimensions on a lattice with site disorder is studied by applying Monte Carlo simulation techniques. Two cases for the site disorder are considered: uncorrelated disorder and long-range correlated disorder with a spatial correlation function that decays according to a power law  $r^{-a}$ . The critical exponents  $\beta$  and  $\gamma$  as well as updated results for the critical exponent  $\nu$  and confluent correction exponent  $\omega$  are provided for a variety of different correlation exponents  $a$  and disorder concentrations  $p_d$ . The estimation is done by using finite-size scaling analyses and a global fit procedure which combines the results obtained for different concentrations of defects. From the estimated critical exponents, the validity of hyperscaling relations is studied and finally the critical temperatures are provided for different  $a$  and  $p_d$ .

 DOI: [10.1103/PhysRevB.105.214111](https://doi.org/10.1103/PhysRevB.105.214111)

## I. INTRODUCTION

Pure materials without any impurities and distortions are seldom found in nature. Often, a certain disorder can be observed. This can be, e.g., structural displacements or point defects in the atomic lattice. Thus, understanding the influence of disorder on the behavior of a system is of a big importance. The goal of this paper is to study the influence of quenched site disorder on the phase transition behavior of an Ising model. We distinguish between two different disorder cases. In the *uncorrelated disorder* case, we place random defects (vacant sites) on the Ising model lattice. Contrarily, in the case of *correlated disorder* we additionally impose a spatial correlation between the defects. In this paper, we assume a power-law decay of the correlation function between the defects.

One of the key achievements for the uncorrelated disorder case is the *Harris criterion* [1], which couples the influence of the disorder on the critical behavior of a system to its specific heat critical exponent in the pure case, i.e.,  $\alpha_{\text{pure}}$ . It states that the disorder is not relevant for systems with  $\alpha_{\text{pure}} < 0$ . Contrarily, if  $\alpha_{\text{pure}} > 0$ , the disorder is relevant and the disordered system will change its universality class, i.e., will have a new set of critical exponents. The Harris criterion is widely accepted and was solidified in various works, in particular, for the case of the three-dimensional Ising model with the help of Monte Carlo techniques [2–7]

and renormalization group calculations [8–11]. The results are also in agreement with experimental data for disordered Ising-like systems [12–16]. A comprehensive review comparing the results from Monte Carlo simulations, renormalization group calculations, and experiments is Ref. [17]. For the two-dimensional Ising model, the Harris criterion does not predict the expected behavior since in this case the Ising model has  $\alpha_{\text{pure}} = 0$ . It is widely accepted that the universality class does not change, but additional logarithmic corrections to scaling have to be considered.

For the correlated disorder case, the *extended Harris criterion* was derived by Weinrib and Halperin [18]. They used a renormalization group  $\epsilon$ - $\delta$ -expansion with  $\epsilon = 4 - d$  and  $\delta = 4 - a$  and showed the following relation. When the disorder is correlated according to a power law  $r^{-a}$ , then the disorder correlation is relevant and leads to a new universality class if the correlation exponent satisfies  $a < d$ , i.e., the correlation is strong enough. Otherwise, for  $a \geq d$ , the standard Harris criterion is recovered and the system behaves effectively as in the uncorrelated disorder case. Weinrib and Halperin also made a conjecture in Ref. [18]: They claim that for the Ising model with correlated disorder, the critical exponent of the correlation length will obey

$$\nu = \frac{2}{a}. \quad (1)$$

This conjecture is not proven in Ref. [18]. The authors also state that  $a \approx 4$  is a necessary condition for the results to hold. Nevertheless, Honkonen and Nalimov [19] claim that the conjecture is exact to all orders of the  $\epsilon$ - $\delta$ -expansion. This was further discussed in Refs. [20,21]. In Ref. [18], the authors also provide estimates for other critical exponents, namely,

$$\alpha = \frac{2(a - d)}{a}, \quad (2)$$

\*physics@kazmin.de

TABLE I. Summary of the critical exponents from various works dealing with the uncorrelated and long-range correlated disordered Ising model in three dimensions. For comparison, recent high-precision estimates for the pure Ising model are also provided. FSS: data analyzed with finite-size scaling, TS: data analyzed with temperature scaling, CB: conformal bootstrap calculations, MC: Monte Carlo simulations, RG: renormalization group calculations, FFM: long-range correlated disorder generated with Fourier filter method, and DL: long-range correlated disorder reached by using lines of disorder.

Ref.	$a$	$\nu$	$\eta$	$\alpha$	$\beta$	$\gamma$	$\omega$	$p_d$	No. $p_d$	Notes
Pure Ising model										
CB [43]	$\infty$	0.629971(4)	0.0362978(20)	0.11009(2) <sup>b</sup>	0.326419(3) <sup>b</sup>	1.237075(10) <sup>b</sup>	0.82968(23)			
MC [44]	$\infty$	0.629912(86)	0.03610(45) <sup>b</sup>	0.11026(26) <sup>b</sup>	0.32630(22)	1.23708(33)	0.83 <sup>e</sup>			FSS
Uncorrelated disorder										
MC [2]	$\infty$	0.6837(53)	0.0374(45)	-0.051(16) <sup>a</sup>	0.3546(28) <sup>a</sup>	1.342(10) <sup>a</sup>	0.37(6)	0.1–0.6	5	FSS
[3]	$\infty$	0.683(3)	0.035(2)	-0.049(9) <sup>a</sup>	0.3535(17) <sup>a</sup>	1.342(6) <sup>a</sup>		0.2	1	TS
[4]	$\infty$	0.68(2)	0.029(60) <sup>b</sup>	-0.04(6) <sup>b</sup>	0.35(1)	1.34(1)		0.3–0.6	3	FSS, TS
[5]	$\infty$	0.678(6) <sup>c</sup>	0.045(19) <sup>cb</sup>	-0.0216(70) <sup>c</sup>	0.3178(40) <sup>c</sup>	1.3258(40) <sup>c</sup>		0.05–0.4	4	FSS
[6]	$\infty$	0.683(2)	0.036(1)	-0.049(6) <sup>a</sup>	0.354(1) <sup>a</sup>	1.341(4) <sup>a</sup>	0.33(3)	0.2, 0.35	2	FSS
RG [8]	$\infty$	0.671(5)	0.025(10)	-0.0125(80) <sup>a</sup>	0.344(6) <sup>a</sup>	1.325(3) <sup>a</sup>	0.32(6)			5-loop RG expansion
[9]	$\infty$	0.675 <sup>d</sup>	0.049 <sup>d</sup>	-0.026 <sup>d</sup>	0.354 <sup>db</sup>	1.317 <sup>db</sup>	0.39 <sup>d</sup>			4-loop RG expansion
[10]	$\infty$	0.678(10)	0.030(3)	-0.034(30) <sup>a</sup>	0.349(5) <sup>a</sup>	1.330(17)	0.25(10)			6-loop RG expansion
[11]	$\infty$	0.675(19)	0.024(79) <sup>a</sup>	-0.025(58) <sup>a</sup>	0.346(34) <sup>a</sup>	1.334(38)	0.15(10)			6-loop RG expansion
Correlated disorder										
MC [22]	2.0	1.012(16)	0.043(4)	-1.036(48) <sup>b</sup>	0.528(34) <sup>b</sup>	1.980(33) <sup>b</sup>	1.01(13)	0.2, 0.35	2	FSS, FFM, DL
[25]	2.0	0.71(1)	-0.030(36) <sup>b</sup>	-0.078(30)	0.362(20)	1.441(15)	0.76(5) <sup>e</sup>	0.2	1	FSS, DL
[23]	2.0	0.958(4)	0.191(18) <sup>b</sup>	-0.789(3) <sup>b</sup>	0.528(3)	1.733(11)	0.8 <sup>e</sup>	0.2	1	FSS, DL
RG [18]	$a < d$	$2/a$	$O(\epsilon^2)^f$	$2(a-d)/a^f$	$(2-\epsilon)/a + O(\epsilon^2)^f$	$4/a + O(\epsilon^2)^f$				2-loop $\epsilon$ - $\delta$ -expansion
[24]	3.0	0.6715	0.0327	-0.014 <sup>b</sup>	0.347 <sup>b</sup>	1.321 <sup>b</sup>				Scaling functions
	2.5	0.7046	0.0118	-0.114 <sup>b</sup>	0.3565 <sup>a</sup>	1.4008 <sup>a</sup>				In 2-loop
	2.0	0.715	-0.0205	-0.147 <sup>b</sup>	0.34 <sup>b</sup>	1.4456 <sup>b</sup>				Approximation

<sup>a</sup>Calculated from other exponents through scaling relations in the original work.

<sup>b</sup>Calculated from other exponents through scaling relations by us.

<sup>c</sup>Averaged over various  $p_d$  by us (weighted mean).

<sup>d</sup>Error is stated to be around several percent.

<sup>e</sup>Not measured (fixed value or the one which gives best fits).

<sup>f</sup>Stated in the paper as an expression for the case where the dimension of the order parameter is  $m > 1$ .

$$\beta = \frac{2-\epsilon}{a} + O(\epsilon^2), \quad (3)$$

$$\gamma = \frac{4}{a} + O(\epsilon^2). \quad (4)$$

However, these relations are given for the case of models with an order parameter with a dimension larger than one. It is unclear from the text whether they are supposed to be valid in the case of one-dimensional order parameter model as is the case for the Ising model. Nevertheless, in this paper we will compare our results for the critical exponents  $\beta$  and  $\gamma$  to Eq. (3) and Eq. (4), respectively.

Contrary to the uncorrelated case, the results for the correlated disorder case in the literature are contradictory. While in Refs. [22,23] the prediction given in Eq. (1) is supported at least qualitatively, in Refs. [24,25] the authors get completely different results for  $\nu$  using both Monte Carlo and renormalization group techniques. Motivated by this discrepancy, we studied the model once again in Ref. [7]. We determined the critical exponent  $\nu$  and our outcome was that it matches the proportionality  $\propto 1/a$  but Eq. (1) is not matched exactly. Additionally, the confluent correction exponent  $\omega$  as well as the critical temperatures in dependence of the concentration

of defects  $p_d$  and the correlation exponent  $a$  were calculated in Ref. [7] and a dedicated analysis of the underlying disorder generation process and the resulting disorder realizations was provided.

In this paper, we extend our analysis of the correlated disorder Ising model and derive the critical exponents  $\beta$  and  $\gamma$ . We will also present improved results for the exponent  $\nu$  and the correction exponent  $\omega$  as compared to Ref. [7] as well as more precise estimates for the critical temperatures. This was possible since we included more simulation temperatures and thereby were able to get the observable peaks more accurately.

As a final introductory remark, we note that site disorder is not the only option to introduce disorder on the lattice. Another possibility is bond disorder. It can be understood as a random coupling between the sites  $J_{x,y}$  which can take different values. Such models were studied, e.g., in Refs. [26–28]. Finally, the two-dimensional Ising model with uncorrelated site or bond disorder cases was studied multiple times, e.g., in Refs. [29–40] while the correlated case was investigated in, e.g., Refs. [41,42]. We compile the critical exponents as well as some further details for the three-dimensional Ising model with uncorrelated and correlated disorder obtained by various groups in Table I.

The rest of this paper is structured as follows. In Sec. II, we will present the studied model and define the necessary notation. We will also briefly sketch the analysis process and give the details of the performed simulations. In Sec. III, we will provide updated results for the critical exponent  $\nu$  and the confluent correction exponent  $\omega$ . After that, we will derive the critical exponents  $\beta$  and  $\gamma$  by using finite-size scaling analysis and, finally, examine the validity of the hyperscaling relations for different  $a$ . In Sec. IV, we will summarize and discuss the results of this paper. In particular, the conjecture by Weinrib and Halperin will be addressed.

## II. MODEL AND SIMULATION DETAILS

### A. Ising model with site disorder

The Hamiltonian of the Ising model with site disorder is given by

$$\mathcal{H} = -J \sum_{\langle xy \rangle} \eta_x \eta_y s_x s_y - h \sum_x \eta_x s_x, \quad (5)$$

where the spins can take the values  $s_x = \pm 1$  and the first sum runs over all nearest neighbors (denoted by  $\langle xy \rangle$ ) of a three-dimensional simple-cubic lattice of size  $V = L^3$  with periodic boundary conditions. The defect variables are  $\eta_x = 1$  when a spin is present at site  $x$  and  $\eta_x = 0$  when site  $x$  is empty. The coupling constant is set to  $J = 1$ , fixing the energy scale, and no external magnetic field is applied, i.e.,  $h = 0$ . For a more detailed description of the (pure) Ising model, we refer to, e.g., Refs. [45,46].

In this paper, we consider two different disorder types. The first type is *uncorrelated disorder* or random disorder. In this case, the defects are chosen randomly according to the probability density

$$f(\eta) = p\delta(\eta) + p_d\delta(\eta - 1), \quad (6)$$

where  $p$  is the concentration of spins,  $p_d = 1 - p$  is the concentration of defects, and  $\delta$  is the Dirac-delta distribution.

The second type is *correlated disorder*. Here, the probability density is still given by Eq. (6), but additionally the spatial correlation between the defects decays according to a power law,

$$\langle \eta_x \eta_y \rangle \propto \frac{1}{r(x, y)^a}, \quad (7)$$

where  $r(x, y)$  is the distance between sites  $x$  and  $y$  and  $a \geq 0$  is the *correlation exponent*. In both cases, we use the grand-canonical approach where the desired concentration of defects  $p_d$  is a mean value over all realizations. Examples of slices of the Ising model lattice for different concentrations of defects  $p_d$  and different correlation exponents  $a$  are presented in Fig. 1. They were taken from a simulation near the corresponding critical temperatures. The expected universality classes for the three-dimensional Ising model according to the Harris criterion and the extended Harris criterion discussed above are schematically shown in Fig. 2.

### B. Long-range site disorder generation

In this paper, we use the *Fourier filter method* for the generation of long-range power-law correlated site disorder. It was

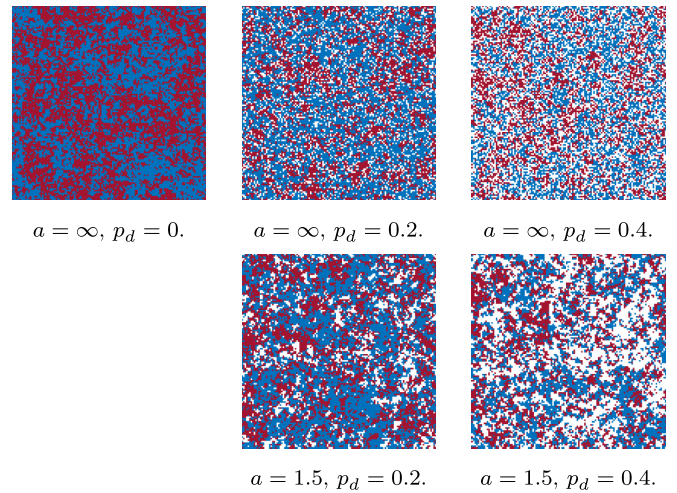


FIG. 1. Slices of a three-dimensional Ising model lattice with  $L = 128$  simulated near the critical temperature for different correlation exponents  $a$  and concentrations of defects  $p_d$ . Red and blue points represent the spin states  $s_x = \pm 1$  and white points represent the defects  $\eta_x = 0$ . One can see that correlated defects tend to form clusters of defects. Taken from Ref. [7].

first introduced by Makse *et al.* [48], but we used a slightly modified version presented in Ref. [47] and the implementation therein. For technical reasons, the imposed correlation function in the method of Ref. [47] is not the power law but a slightly modified function of the form  $C(r) = (1 + r^2)^{-2/a}$ . This fact and also the presence of finite-size effects make the measurement of the true correlation exponents  $\bar{a}$  after the generation process an important analysis step. We carefully determined the  $\bar{a}$  in Ref. [7] and compile these values in Table II. For details of the generation of correlated disorder, we refer to Ref. [7].

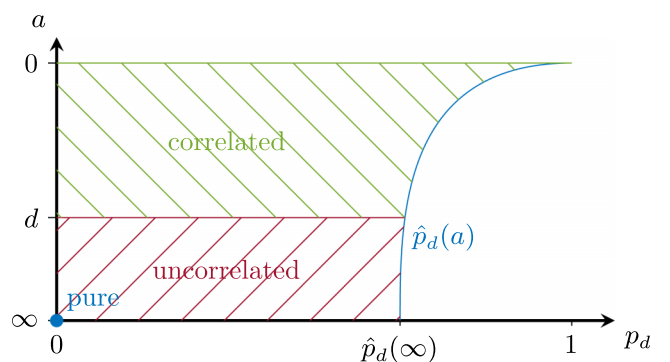


FIG. 2. Universality classes of the three-dimensional Ising model for different correlation exponents  $a$  and concentrations of defects  $p_d$ . The curve  $\hat{p}_d(a) = 1 - \hat{p}_d(a)$  is the percolation threshold of the defect concentration below which an infinite spin cluster exists for  $L \rightarrow \infty$ . It has been shown in Ref. [47] that for smaller  $a$  values, the concentration of spins  $p$  can be chosen lower without destroying the infinite cluster, thus  $p_d$  increases for stronger correlations (smaller  $a$ ). Taken from Ref. [7].

TABLE II. The measured correlation exponents  $\bar{a}$  from Ref. [7] and updated results of the critical exponent  $\nu$  and the confluent correction exponent  $\omega$ .

$a$	$\bar{a}$	$\nu$	$\omega$
$\infty$		0.6831(30)	0.346(40)
3.5	3.30(18)	0.7117(49)	0.679(44)
3.0	2.910(96)	0.7484(52)	0.840(50)
2.5	2.451(26)	0.8719(96)	1.154(66)
2.0	1.979(18)	1.060(23)	1.087(81)
1.5	1.500(30)	1.421(55)	0.988(75)

### C. Monte Carlo simulation details

The simulations used for this paper were organized as in Ref. [7], but we mention them here briefly for completeness. We performed Monte Carlo simulations of the Ising model with site disorder employing the Swendsen-Wang multiple-cluster update algorithm [49]. The linear lattice sizes of our simple-cubic lattices were in the range between  $L = 8$  and  $L = 256$ , and we chose periodic boundary conditions in each direction. The correlation exponents were  $a = 1.5, 2.0, 2.5, 3.0, 3.5$ , and  $\infty$ , which we will use symbolically for the uncorrelated case. For each  $a$  value, we simulated eight concentrations of defects  $p_d = 0.05, 0.1, 0.15, 0.2, 0.25, 0.3, 0.35$ , and  $0.4$ . We used  $N_c = 1000$  disorder realizations for each parameter tuple  $(a, p_d, L)$  and performed  $N = 10\,000$  measurements after 500 thermalization sweeps for each temperature  $\beta_{\text{sim}}$ . We will use the inverse temperature  $\beta = 1/(k_B T)$  for the rest of the paper and call it simply temperature.<sup>1</sup> We measured the total energy  $E$ ,

$$E = -J \sum_{(xy)} \eta_x \eta_y s_x s_y, \quad (8)$$

and the total magnetization of the system  $M$ :

$$M = \sum_x \eta_x s_x. \quad (9)$$

after each sweep and recorded these values in a time-series file for further analyses.

### D. Analysis process

We would like to briefly repeat the analysis steps which were performed in Ref. [7] and which are discussed there in great detail. We do this, because the analysis steps in this work were identical except for the observables to which they were applied. In our simulations, we used different temperatures with narrow spacing to find the region of the peak of a certain observable  $\mathcal{O}$  for each parameter tuple  $(a, p_d, L)$ . After that, we used the single histogram reweighting technique as described in Ref. [50] (initially introduced in Ref. [51]) to find the peak value  $\hat{\mathcal{O}}$  and the corresponding temperature  $\beta_{\text{max}}$ . To obtain the error of  $\hat{\mathcal{O}}$ , we used a jackknife resampling technique [52,53]. Finally, we used the finite-size scaling method

<sup>1</sup>Note that the inverse temperature and the critical exponent  $\beta$  share the same notation in this paper. However, the correct quantity should always be clear from the context.

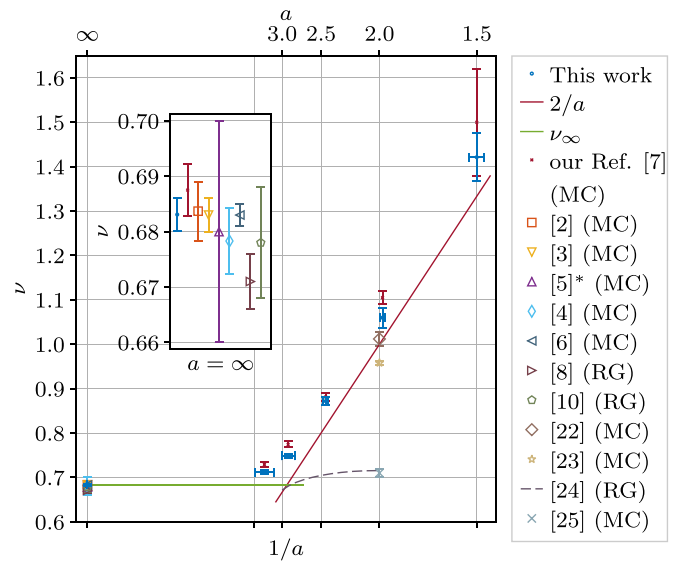


FIG. 3. Updated results for the critical exponent  $\nu$  from Ref. [7]. For our results, we use the measured  $\bar{a}$  values from Table II. The inset shows the uncorrelated case with  $a = \infty$  and  $\nu_\infty$  indicates the average over literature values for the uncorrelated case. MC: Monte Carlo simulations, RG: renormalization group calculations, \*: weighted mean over several  $p_d$ .

to derive the critical exponents from global fits incorporating the results for several disorder concentrations  $p_d$ . The details of the global fit ansatz and jackknife resampling can be found in the Appendix of Ref. [7].

## III. RESULTS

### A. Updated results for exponent $\nu$ and $\omega$

In Ref. [7], we already derived the critical exponent of the correlation length  $\nu$  and the confluent correction exponent  $\omega$  for the Ising model with long-range correlated site disorder. However, recently we were able to further improve the results by simulation at additional temperatures closer to the expected peaks of the studied observables. Therefore, we would like to provide updated results of  $\nu$  and  $\omega$  here, which we will also use in the later analyses in this paper. The results are summarized in Fig. 3 and Table II together with the measured correlation exponents  $\bar{a}$ . For a detailed description of the derivation process, we refer to Ref. [7]. We only would like to mention that  $\nu$  and  $\omega$  were obtained through a finite-size scaling analysis similar to what is described in this paper for the critical exponents  $\beta$  and  $\gamma$ .

The main outcome did not change much compared to Ref. [7]. We see a clear proportionality of  $\nu$  of the form  $1/a$  and expect Eq. (1) to be the leading order. The confluent correction exponent  $\omega$  in the correlated cases is no longer constant but otherwise remains in the same quantitative region. It shows a maximum around  $a = 2.5$ , which is in surprisingly good qualitative agreement with Ref. [54] where the correction exponent was obtained through field-theoretic renormalization group calculations. In the crossover region around  $a \approx 3.0$ , according to Ref. [18] the leading correction exponent should go to zero. Right at the crossover point, it vanishes and one expects the marginal case where

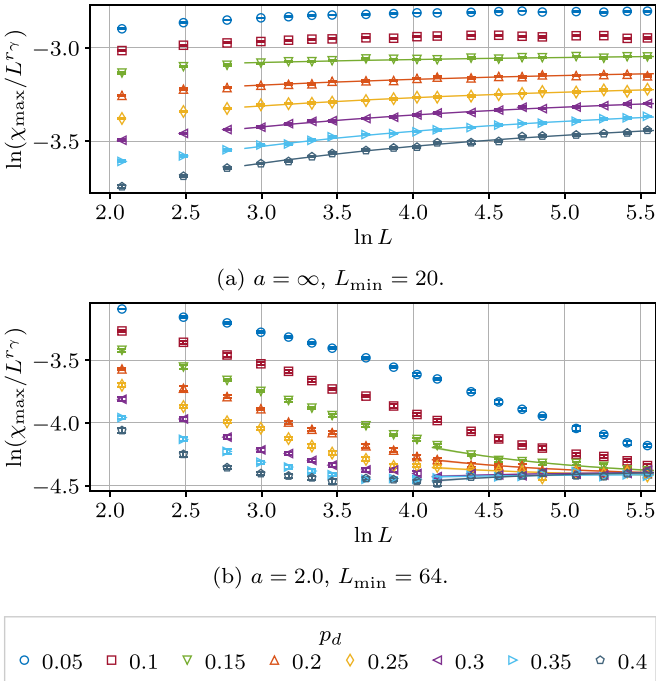


FIG. 4. Examples of the fits to the ansatz in Eq. (12) for two different  $a$  and the corresponding finally chosen  $L_{\min}$ . The values  $\chi_{\max}(L, p_d)$  are scaled by  $L^{r_\gamma}$ , i.e., if there were no corrections to scaling ( $B_{p_d} = 0$ ), the points would lie on a horizontal line in these plots.

corrections-to-scaling might decay only logarithmically in  $L$ . Our  $\omega$  estimate apparently does not support this expectation, but the relatively large deviation of the critical exponent from the prediction  $\nu = 2/a$  indeed reflects strong corrections-to-scaling at the crossover point. It is likely that using a fit ansatz of the form  $AL^{1/\nu}(1 + BL^{-\omega})$ , which was used in Ref. [7], the critical exponent is effectively shifted from its true asymptotic value while the correction exponent obtained from the fit is essentially the exponent of the subleading correction. In fact, the correlated cases with  $a \lesssim d$  should be governed by two different correction-to-scaling terms with quite small correction exponents [18]. Our present data are, however, not precise enough to disentangle this subtle interplay of different correction terms.

### B. Critical exponent $\gamma$

For the derivation of the critical exponent  $\gamma$ , we used the susceptibility  $\chi$  as the observable. It is defined as

$$\chi(\beta) = \beta V([\langle m^2 \rangle] - [\langle |m| \rangle]^2), \quad (10)$$

where  $\langle \cdot \rangle$  and  $[\cdot]$  denote the thermal and disorder averages, respectively. The finite-size scaling behavior of the peaks  $\chi_{\max}(L)$  of  $\chi(\beta)$  for a given lattice size  $L$  is given in leading order by

$$\chi_{\max}(L) = AL^{\gamma/\nu}(1 + BL^{-\omega}), \quad (11)$$

where  $A$  and  $B$  are amplitudes and  $\omega$  is the confluent correction exponent. Because the critical exponents are expected to be independent of the concentration of defects  $p_d$  in the thermodynamic limit, we use a global fit ansatz and combine

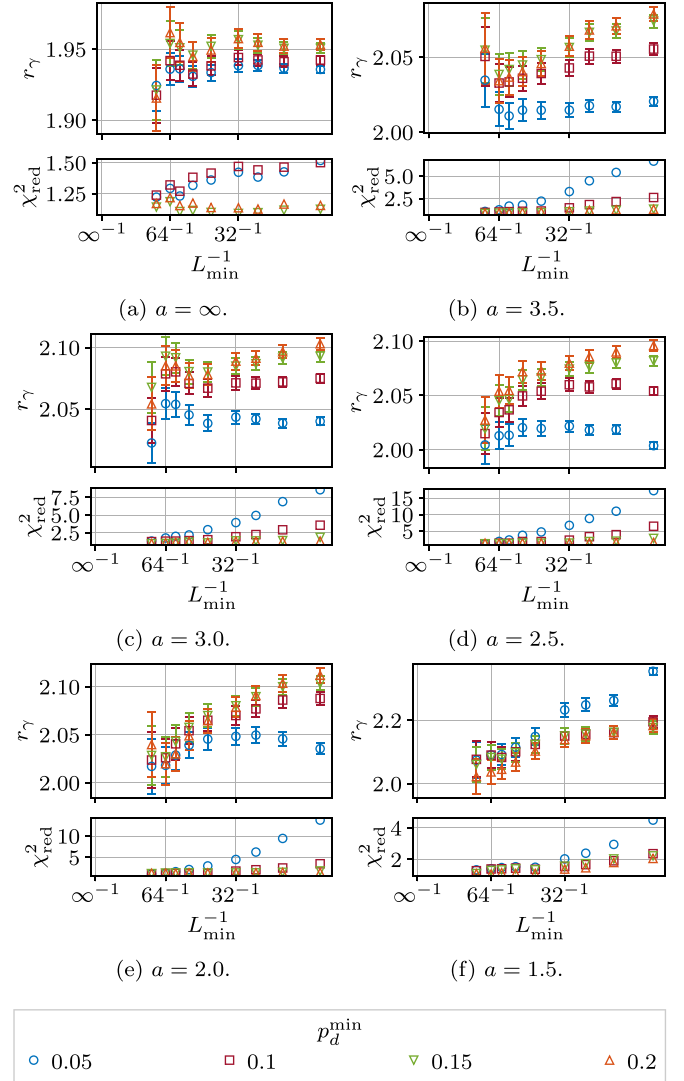


FIG. 5. Fitted ratios  $r_\gamma = \gamma/\nu$  from the fits to the ansatz in Eq. (12), with varying  $p_d^{\min}$  and  $L_{\min}$ . The corresponding qualities of fits  $\chi_{\text{red}}^2$  are shown as a second plot for each  $a$ .

all  $p_d$  in one fit by only letting the amplitudes depend on  $p_d$ , i.e.,

$$\chi_{\max}(L, p_d) = A_{p_d} L^{\gamma/\nu} (1 + B_{p_d} L^{-\omega}), \quad (12)$$

where  $r_\gamma = \gamma/\nu$ , and we fix the correction exponent  $\omega$  to the previously determined estimates from Table II.

We performed least-squares fits with the ansatz in Eq. (12) and varied the minimum concentration of defects  $p_d^{\min}$  and the smallest lattice size  $L_{\min}$ . Two examples of the fits are shown in Fig. 4 and the resulting  $r_\gamma$  are presented in Fig. 5. Including  $p_d = 0.05$  and  $p_d = 0.1$  into the global fit ansatz usually resulted in bad fit qualities reflected by large chi-squared values per degree of freedom  $\chi_{\text{red}}^2$ , and we finally chose  $p_d^{\min} = 0.15$  for all considered cases. Concerning the minimum lattice size, we have chosen the smallest value, where the estimates for  $p_d^{\min} = 0.15$  and  $p_d^{\min} = 0.2$  mostly overlapped due to the size of their errors. This was done to account for the freely adjustable parameter  $p_d^{\min}$ . The finally selected  $L_{\min}$  can be found in Table III.

TABLE III. Results of the critical exponent  $\gamma$ . Additionally, the fit parameters  $r_\gamma$  and the calculated exponents  $\eta$  are provided. The chosen minimum concentration of defects in the fits to ansatz in Eq. (12) was  $p_d^{\min} = 0.15$ .

$a$	$r_\gamma$	$\gamma = r_\gamma \nu$	$\eta = 2 - r_\gamma$	$\chi_{\text{red}}^2$	$L_{\min}$
$\infty$	1.9506(36)	1.3324(64)	0.0494(36)	1.12	20
3.5	2.039(14)	1.451(15)	-0.039(14)	0.87	64
3.0	2.093(16)	1.566(16)	-0.093(16)	0.99	64
2.5	2.045(14)	1.783(24)	-0.045(14)	1.16	64
2.0	2.027(21)	2.149(51)	-0.027(21)	1.29	64
1.5	2.061(56)	2.93(14)	-0.061(56)	1.11	80

Before discussing the estimated critical exponents  $\gamma$ , let us stick to the fitted ratios  $r_\gamma = \gamma/\nu$  for a moment. For the chosen  $L_{\min}$  and  $p_d^{\min}$ , they are shown in Fig. 6 and also listed in Table III for completeness. For the uncorrelated case, we get  $r_\gamma = 1.9506(36)$ . This is in good agreement with other works, e.g., Refs. [4,6]. All ratios for correlated cases are approximately constant with  $r_\gamma \approx 2.05(3)$ . The largest value is at  $a = 3.0$  with  $r_\gamma = 2.093(16)$ .  $r_\gamma = \gamma/\nu > 2.0$  implies a negative exponent  $\eta = 2 - \gamma/\nu < 0$  which is a bit unusual for an Ising model. Nevertheless, such negative values were also observed in Refs. [24,25].<sup>2</sup> Even for the uncorrelated case, the  $p_d$ -dependent estimates of  $\eta$  can be negative [55,56]. Heuer [55] explains the negative  $\eta$  values as being artifacts of a crossover regime between the uncorrelated case and the pure case. It is conceivable that the same could apply to the crossover between the correlated and uncorrelated regimes. This would coincide with our peak in  $r_\gamma$  being at  $a = 3.0$ , which is the crossover region. The error bars of  $r_\gamma$  for  $a \leq 2.0$  are quite large, so the ratios are not unlikely to become less than two with a more precise measurement, e.g., on larger lattice sizes or with more disorder realizations. On the other hand, there is no rigorous statement known to us which would restrict  $\eta > 0$  for variations of the Ising model. In fact,  $\eta < 0$  is known from other systems, like three-dimensional percolation [57,58] or the three-dimensional cubic model [59]. Note, that if Eqs. (1) and (4) hold, they imply  $\eta = 0$ .

Let us now move to the critical exponent  $\gamma$  itself. For the uncorrelated case, we measure a value of  $\gamma = r_\gamma \nu = 1.3324(64)$ , which is in a very good agreement with other works, as can be seen in Fig. 7. Our value is placed between the estimates from Monte Carlo simulations and the renormalization group calculations. For the correlated cases, we see a behavior  $\propto 1/a$  which is clear since we observed approximately constant ratios  $r_\gamma$  and  $\nu \propto 1/a$ . The values follow close to the  $4/a$  line, which is the predicted behavior from Ref. [18], Eq. (4), as discussed in the Introduction. We therefore can assume that Eq. (4) is the leading behavior but needs correction terms, as was the case for the exponent  $\nu$ . Comparing our estimate for the case  $a = 2.0$  with other groups, we cannot see any agreement. The reason for this

<sup>2</sup>However, due to the discrepancies in the estimates for the critical exponent  $\nu$  between Refs. [24,25] and our paper, their estimates for  $\gamma$  do not coincide with our paper.

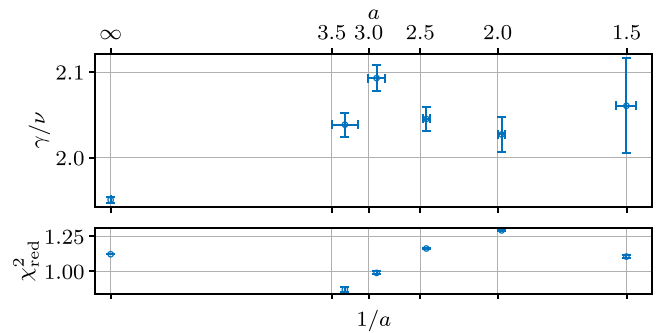


FIG. 6. Ratios  $\gamma/\nu = r_\gamma$  for various correlation exponents  $a$ . Except for the uncorrelated case with  $a = \infty$ , the ratios are  $\gamma/\nu > 2$  which implies  $\eta < 0$ .

discrepancy remains unclear to us, but it is noticeable that the deviations are comparable to the estimates for the exponent  $\nu$  (Fig. 3). It indicates a systematic difference between our analysis and other works, one of which is our usage of a global fit approach.

### C. Critical exponent $\beta$

In contrast to most other works listed in Table I where the critical exponent  $\beta$  was only calculated through scaling relations, we performed a dedicated analysis and obtained independent estimates for  $\beta$ . The estimation of the critical exponent  $\beta$  was done along the same lines as for  $\gamma$ . Here, the observable of interest is the derivative with respect to  $\beta$  of the magnetization:

$$\partial_\beta \langle |m| \rangle (\beta) = \frac{\partial}{\partial \beta} \langle |m| \rangle = V(\langle |m| \rangle \langle e \rangle - \langle |m| e \rangle). \quad (13)$$

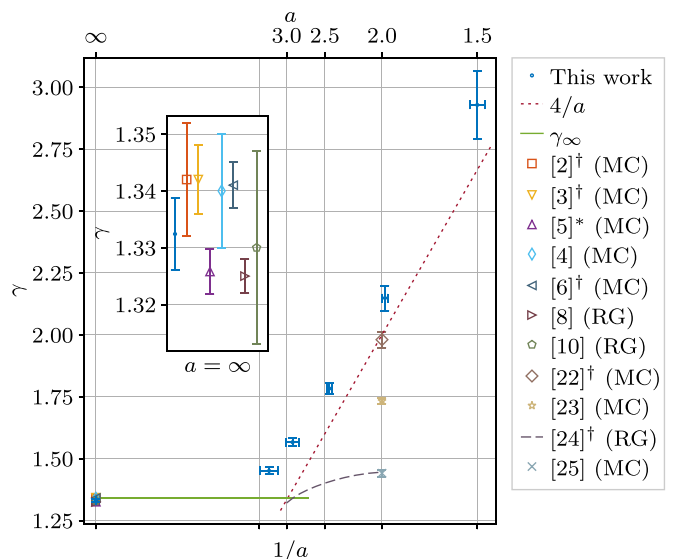


FIG. 7. Results of the critical exponent  $\gamma$  compared to the literature. For our results we use the measured  $\bar{a}$  values from Table II. The inset shows the uncorrelated case with  $a = \infty$  and  $\gamma_\infty$  indicates the average over literature values for the uncorrelated case. MC: Monte Carlo simulations, RG: renormalization group calculations, †: calculated from  $\eta$  and  $\nu$ , \*: weighed mean over several  $p_d$ .

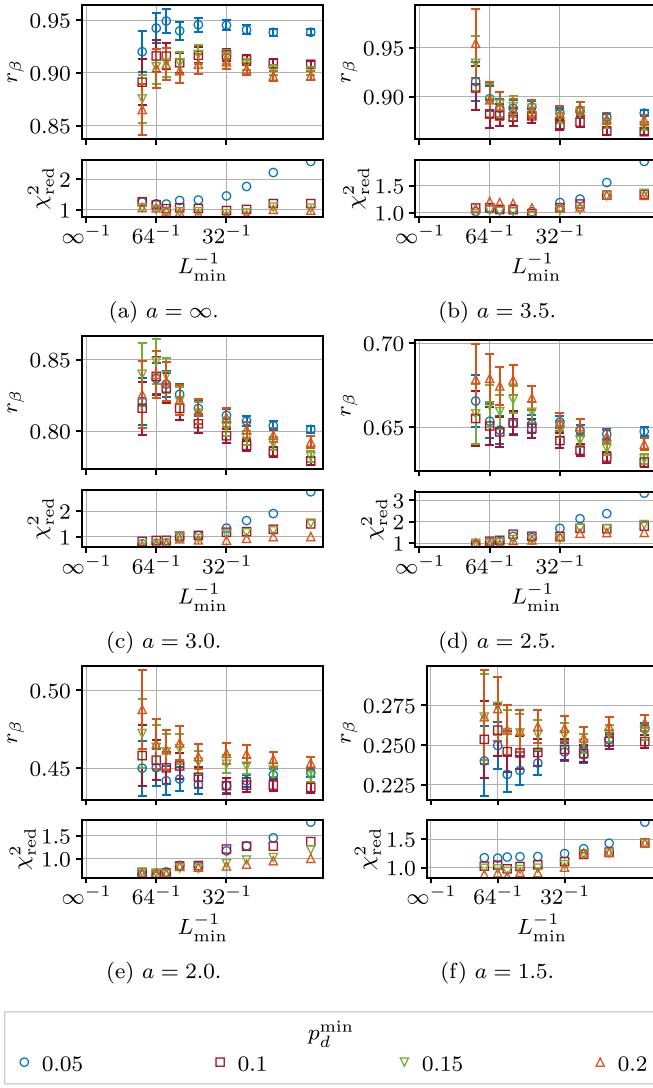


FIG. 8. Fitted ratios  $r_\beta = (1 - \beta)/\nu$  from the fits to the ansatz in Eq. (15), with varying  $p_d^{\min}$  and  $L_{\min}$ . The corresponding qualities of fits  $\chi_{\text{red}}^2$  are shown as a second plot for each  $a$ .

The finite-size scaling behavior of the peaks  $\partial_\beta(|m|)_{\max}(L)$  of  $\partial_\beta(|m|)(\beta)$  for a given lattice size  $L$  in leading order is [60]

$$\partial_\beta(|m|)_{\max}(L) = AL^{(1-\beta)/\nu}(1 + BL^{-\omega}). \quad (14)$$

Using the global ansatz for all  $p_d$ , we get

$$\partial_\beta(|m|)_{\max}(L, p_d) = A_{p_d}L^{r_\beta}(1 + B_{p_d}L^{-\omega}), \quad (15)$$

where  $r_\beta = (1 - \beta)/\nu$ . As previously, we fixed the correction exponent  $\omega$  in the fits with Eq. (15) and varied the minimum concentration of defects  $p_d^{\min}$  and the smallest lattice size  $L_{\min}$ . We present the results for  $r_\beta$  for all considered  $p_d^{\min}$  and  $L_{\min}$  in Fig. 8. Two examples of global fits with the ansatz in Eq. (15) are shown in Fig. 9.

Concerning the minimum concentration of defects,  $p_d^{\min} = 0.15$  was a good choice as in the case for the exponent  $\gamma$ . This was the lowest possible value which gave reasonable fit qualities  $\chi_{\text{red}}^2 \approx 1$ . For the minimum lattice size, it was

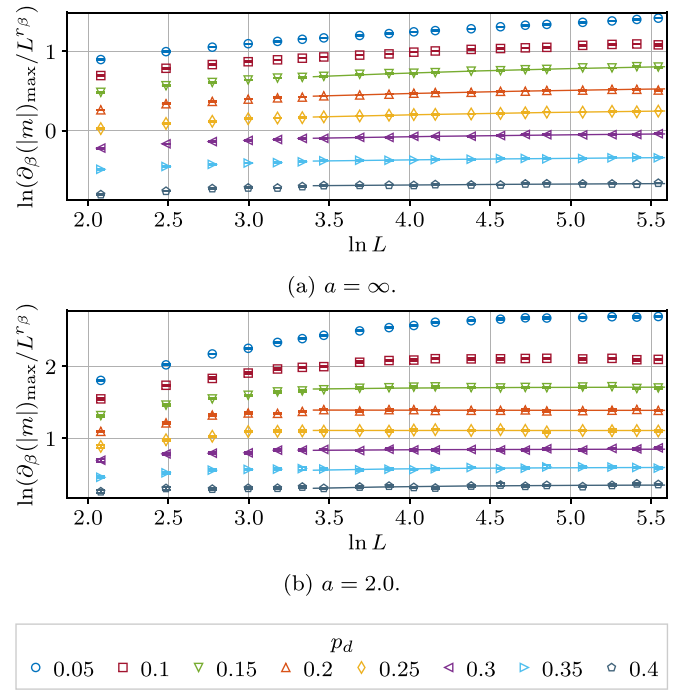


FIG. 9. Examples of the fits to the ansatz in Eq. (15) for two different  $a$  and the corresponding finally chosen  $L_{\min} = 32$ . The values  $\partial_\beta(|m|)_{\max}(L, p_d)$  are scaled by  $L^{r_\beta}$ , i.e., if there were no corrections to scaling ( $B_{p_d} = 0$ ), the points would lie on a horizontal line in these plots.

possible to select one value  $L_{\min} = 32$  for all considered cases. The final results are summarized in Fig. 11 and Table IV.

Before going into the discussion of the estimated critical exponents  $\beta$ , we would like to take a look at the ratios  $\beta/\nu$  as we have done for the exponent  $\gamma$ . Unfortunately, the fit parameter in the ansatz was  $r_\beta = (1 - \beta)/\nu$ , so the ratios  $\beta/\nu$  were not directly measured but calculated by

$$\frac{\beta}{\nu} = r_\nu - r_\beta, \quad (16)$$

$$\epsilon\left(\frac{\beta}{\nu}\right) = \sqrt{\epsilon(r_\nu)^2 + \epsilon(r_\beta)^2}, \quad (17)$$

where  $\epsilon$  denotes the errors and  $r_\nu = 1/\nu$  are the fitted ratios for the exponent  $\nu$ . The ratios are listed in Table IV and shown in Fig. 10. Again, we can observe an approximately constant value of  $\beta/\nu \approx 0.51(3)$  for all correlated cases except for

TABLE IV. Results of the critical exponent  $\beta$ . Minimum concentration of defects was  $p_d = 0.15$  and minimum lattice size was  $L_{\min} = 32$ .

$a$	$r_\beta$	$\frac{\beta}{\nu} = \frac{1}{\nu} - r_\beta$	$\beta = 1 - r_\beta \nu$	$\chi_{\text{red}}^2$
$\infty$	0.9151(66)	0.5488(92)	0.3749(53)	0.88
3.5	0.8794(66)	0.526(12)	0.3741(64)	1.05
3.0	0.8026(60)	0.534(11)	0.3993(61)	1.12
2.5	0.6487(48)	0.498(14)	0.4344(75)	1.20
2.0	0.4526(59)	0.491(21)	0.520(12)	0.90
1.5	0.2565(73)	0.447(28)	0.635(18)	1.05

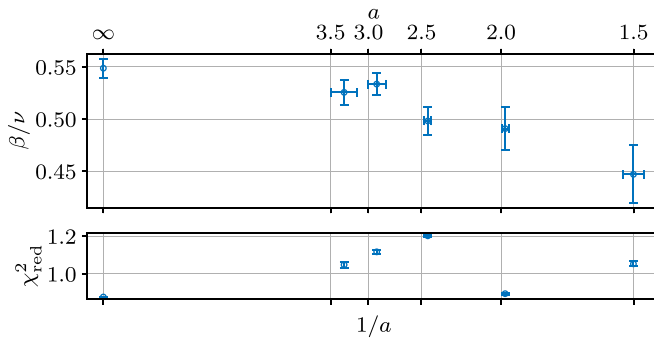


FIG. 10. Ratios  $\beta/\nu$  for various correlation exponents  $a$ . For all correlated cases except for  $a = 1.5$ , an approximately constant value can be seen.

$a = 1.5$ , which clearly deviates from this behavior. The value for the uncorrelated case with  $\beta/\nu = 0.5488(92)$  is also close to this constant. Using Eq. (1) and assuming Eq. (3) to be valid, we would expect a constant ratio of  $\beta/\nu = 1/2$ . Our results get reasonably close to it.

Comparing the estimate for exponent  $\beta$  in the uncorrelated case, we see a clear deviation from all other groups. It has to be mentioned, though, that most of the other groups did not measure  $\beta$  directly but instead calculated it from  $\nu$  and  $\gamma$  by using scaling relations (see Table I and marks in Fig. 11). Therefore, the comparison is a bit vague. In our opinion, there is no clear reason why our estimate deviates that much from other groups since the fit quality is good and also the fitted data look reasonably well (see Fig. 9). The result for  $p_d^{\min} = 0.05$  is much closer to other groups but because it does not overlap with the results for higher  $p_d^{\min}$ , we expect it to be influenced by a crossover to the pure Ising model case.

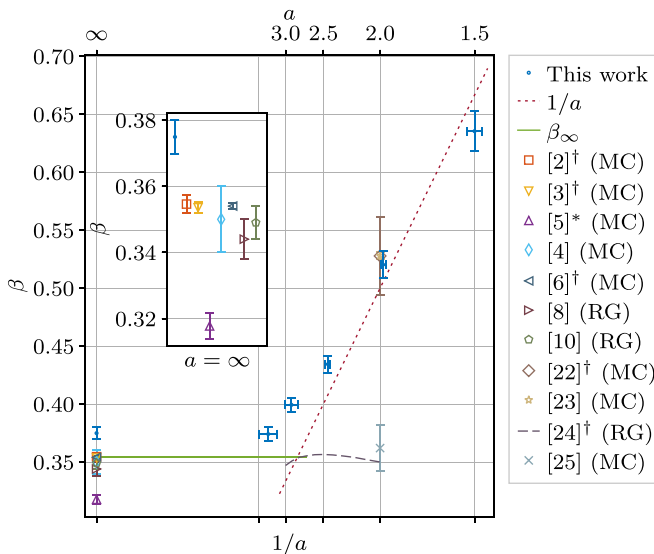


FIG. 11. Results of the critical exponent  $\beta$  compared to the literature. For our results, we use the measured  $\bar{a}$  values from Table II. The inset shows the uncorrelated case with  $a = \infty$  and  $\beta_\infty$  indicates the average over literature values for the uncorrelated case. MC: Monte Carlo simulations, RG: renormalization group calculations, †: calculated from  $\gamma$  and  $\nu$ , \*: weighed mean over several  $p_d$ .

In the correlated cases, we observe a slightly different behavior than for  $\nu$  and  $\gamma$ . The deviation of  $\beta$  from  $1/a$  is significant for large  $a$  while at  $a = 2.0$   $\beta \approx 1/a$  and for  $a = 1.5$  it even goes below  $1/a$ . This behavior is also reflected in the ratios in Fig. 10 which are not quite as constant as  $\gamma/\nu$  were. Considering the relatively large error for the strongest correlated case with  $a = 1.5$ , it is possible that we see an asymptotic behavior in  $\beta$  approaching  $1/a$  for decreasing  $a$ . Once again, this would be a consequence of the crossover regime around  $a \approx 3.0$ . These observations suggest that  $\beta = 1/a$  is the leading behavior, which, however, is affected by even stronger corrections than for  $\nu$  and  $\gamma$ . A further supporting reason for a stronger correction is the presence of the  $\epsilon$  in Eq. (3) while the exponents  $\nu$  and  $\gamma$  have only higher-order corrections of  $O(\epsilon^2)$ .

#### D. Hyperscaling validation

As we know from theory, two critical exponents already completely describe the universality class of a system and all other exponents can be calculated by using scaling or hyperscaling relations. As we are equipped with three exponents, i.e.,  $\nu$ ,  $\gamma$ , and  $\beta$ , we can check them for consistency. In particular, Josephson's law [61,62] and Rushbrooke's law [63], i.e.,

$$d\nu = 2 - \alpha, \quad (18)$$

$$2\beta + \gamma = 2 - \alpha, \quad (19)$$

respectively, can be combined to obtain

$$2\beta + \gamma = d\nu. \quad (20)$$

Note, that Eqs. (18) and (20) are called *hyperscaling relations* since they incorporate the dimensionality  $d$  of the system. As we initially measured ratios instead of the critical exponents themselves, it is advisable to reformulate Eq. (20) to use them and not the final exponents which implicitly also suffer from the error of the critical exponent  $\nu$ . We can write Eq. (20) as

$$2\left(\frac{1}{\nu}\right) - 2\left(\frac{1-\beta}{\nu}\right) + \left(\frac{\gamma}{\nu}\right) \stackrel{?}{=} d, \quad (21)$$

and check its validity for our three-dimensional case  $d = 3$ . Note that in Eq. (21) all three terms in round brackets are the directly fitted parameters, i.e.,  $r_\nu$ ,  $r_\beta$ , and  $r_\gamma$ , respectively. We show the results for all considered  $a$  in Fig. 12.

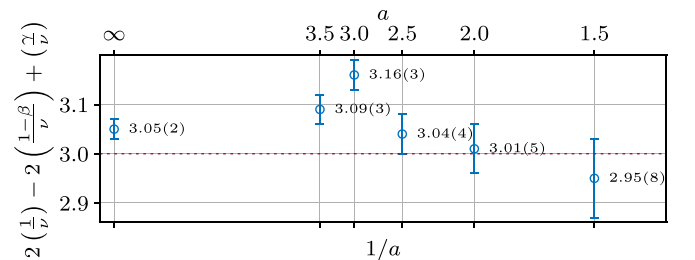


FIG. 12. Check of the hyperscaling relation from Eq. (21) for various considered correlation exponents  $a$ . The expected value is the dimension of the system under consideration, i.e.,  $d = 3$  in this work.

Starting with the uncorrelated case, we observe a value of 3.05(2) which is slightly larger than  $d = 3$  but, within error bars, still compatible. We argue that this slight deviation has the same origin as for the  $\beta$  exponent which is larger than the one calculated by other groups. We would not consider our result to suggest a hyperscaling violation in the uncorrelated disorder case. Contrarily, in the crossover region  $a \approx 3.0$ , we see a larger deviation between calculated values and the expected value for  $d = 3$ . For the strongest correlations with  $a \leq 2.5$ , the results become compatible with the expectation again. Combining the above observations, we arrive at the conjecture that the hyperscaling relation may be violated or be a consequence of strong corrections as discussed in Sec. III C in the crossover region between the (effectively) uncorrelated and correlated cases and is valid otherwise.

### E. Critical temperatures

During the analysis process, we estimated the peaks  $\hat{\mathcal{O}}$  of three observables, namely,  $\partial_\beta(\ln |m|)$ ,  $\partial_\beta(|m|)$ , and  $\chi$  for all parameter tuples  $(a, p_d, L)$ . Alongside these values, we also got the corresponding temperatures  $\beta_{\mathcal{O},\max}$  at which the peaks occurred. These temperatures obey a finite-size scaling relation (neglecting correction terms) of the form

$$\beta_{\mathcal{O},\max}(L) = \beta_c + AL^{-1/\nu}. \quad (22)$$

By combining the estimates  $\beta_{\mathcal{O},\max}(L)$  for all considered observables into one global fit ansatz

$$\beta_{\mathcal{O},\max}(L) = \beta_c + A_{\mathcal{O}}L^{-1/\nu}, \quad (23)$$

with the amplitudes  $A_{\mathcal{O}}$  being dependent on  $\mathcal{O}$ , we get an estimate for the critical temperature  $\beta_c$  for each correlation exponent  $a$  and concentration of defects  $p_d$ . In Eq. (23), we used our previously estimated critical exponent  $\nu$  as a fixed parameter. To account for the error  $\epsilon(\nu)$ , we additionally performed each fit also with  $\nu \rightarrow \nu \pm \epsilon(\nu)$  and included the larger of the two deviations,

$$\epsilon_\nu(\beta_c) = \max_{\nu \pm \epsilon(\nu)} |\beta_c(\nu) - \beta_c(\nu \pm \epsilon(\nu))|, \quad (24)$$

as an additional contribution<sup>3</sup> to the total error

$$\epsilon(\beta_c) = \sqrt{\epsilon_{\text{fit}}(\beta_c)^2 + \epsilon_\nu(\beta_c)^2}, \quad (25)$$

where  $\epsilon_{\text{fit}}(\beta_c)$  is the fit error. Through the usage of the single histogram reweighting technique, intrinsically each  $\beta_{\mathcal{O},\max}(L)$  was more or less precise, depending on how close the simulation temperature  $\beta_{\text{sim}}$  was to the finally found  $\beta_{\mathcal{O},\max}(L)$ . This effect was mostly pronounced for larger concentrations and stronger correlations due to the larger variation of the critical temperatures for each individual disorder realization. This made it impossible to study corrections-to-scaling terms and also made the choice of  $L_{\min}$  less important. Our final choice was  $L_{\min} = 32$ .

The usage of the global fit ansatz in Eq. (23) is an improvement over the estimation which we carried out in Ref. [7],

<sup>3</sup>This proved to provide the same error estimates as the bootstrap method which we used in Ref. [7] but with less effort.

TABLE V. Critical temperatures  $\beta_c$  obtained from global fits including all considered observables to the finite-size scaling ansatz given in Eq. (22). The second number given is the quality of the fit  $\chi_{\text{red}}^2$ .

$p_d$	$a = \infty$		$a = 3.5$		$a = 3.0$	
0.05	0.2345923(3)	2.6	0.2324144(4)	2.4	0.2316970(5)	2.4
0.1	0.2492899(3)	2.1	0.2431346(5)	3.1	0.2413960(8)	1.6
0.15	0.2661580(3)	2.2	0.2546172(7)	1.2	0.251678(2)	1.4
0.2	0.2857454(5)	1.1	0.2673096(9)	0.8	0.262985(2)	1.6
0.25	0.3088137(6)	1.7	0.281652(2)	1.3	0.275679(2)	1.3
0.3	0.3364315(7)	1.1	0.298162(2)	1.2	0.290219(3)	1.3
0.35	0.3701800(9)	1.3	0.317580(2)	1.4	0.307232(4)	1.7
0.4	0.412513(2)	1.7	0.340913(3)	1.8	0.327603(4)	1.7
$p_d$	$a = 2.5$		$a = 2.0$		$a = 1.5$	
0.05	0.230679(1)	1.1	0.229204(4)	1.7	0.22717(2)	4.4
0.1	0.239069(2)	1.0	0.235935(7)	1.3	0.23196(2)	3.4
0.15	0.247880(3)	1.5	0.243025(9)	1.6	0.23700(3)	4.0
0.2	0.257528(3)	2.3	0.250714(7)	3.2	0.24243(3)	9.0
0.25	0.268290(4)	1.9	0.25935(2)	4.3	0.24877(2)	6.6
0.3	0.280630(5)	1.7	0.26916(2)	2.2	0.25599(4)	6.6
0.35	0.294890(7)	2.7	0.28046(2)	5.1	0.26414(4)	23.5
0.4	0.311875(8)	4.1	0.29414(2)	11.8	0.27357(3)	12.1

where we considered only one observable  $\mathcal{O} = \partial_\beta(\ln |m|)$ . The critical temperatures are compiled in Table V together with the corresponding qualities of the global fits  $\chi_{\text{red}}^2$ , which we should carefully examine first. In general, the quality of the fits is reasonably good. However, for the two strongest correlation cases with  $a = 2.0$  and  $a = 1.5$ , the quality is bad for larger concentrations. Therefore, for these two cases our estimates should be considered with great care. Our estimates of the temperatures for the uncorrelated disorder case are in excellent agreement with Refs. [2,6]. We also agree on less accurate estimates from Refs. [3,5]. This is an important verification of the estimation process. Note that all the references stated above used site disorder. For bond disorder, e.g., Ref. [4], the temperatures are different. For the correlated cases, the critical temperatures depend on the correlation exponent  $a$  and on the concentration of defects  $p_d$  but additionally also on the disorder generation method. In particular, line defects (which correspond to  $a = 2.0$  in three dimensions) and pointlike methods (e.g., the Fourier filter method used in this paper) do not share a common critical temperature for  $a = 2.0$  and the same  $p_d$  [22]. Further, using the Fourier filter method one still has various technical parameters like the form of the correlation function and the mapping procedure from continuous to discrete values which influence the critical temperature. All these nuances in the disorder generation make our temperature estimates for the correlated cases incomparable with other works.

## IV. CONCLUSIONS

In this paper, we have studied the three-dimensional Ising model on simple-cubic lattices with long-range power-law correlated ( $\propto r^{-a}$ ) site disorder. The main purpose of this paper was to estimate the missing critical exponents  $\beta$  and

TABLE VI. Complete list of measured critical exponents and exponents calculated through scaling relations (marked with †). Additionally, the confluent correction exponents  $\omega$  and the measured correlation exponents  $\bar{a}$  from Ref. [7] are listed.

$a$	$\bar{a}$	$\nu$	$\gamma$	$\beta$
$\infty$	–	0.6831(30)	1.3324(64)	0.3749(53)
3.5	3.30(18)	0.7117(49)	1.451(15)	0.3741(64)
3.0	2.910(96)	0.7484(52)	1.566(16)	0.3993(61)
2.5	2.451(26)	0.8719(96)	1.783(24)	0.4344(75)
2.0	1.979(18)	1.060(23)	2.149(51)	0.520(12)
1.5	1.500(30)	1.421(55)	2.93(14)	0.635(18)
$a$	$\alpha^\dagger = 2 - d\nu$	$\eta^\dagger = 2 - \gamma/\nu$	$\delta^\dagger = \gamma/\beta + 1$	$\omega$
$\infty$	-0.0493(90)	0.0494(36)	4.554(53)	0.346(40)
3.5	-0.135(15)	-0.039(14)	4.878(76)	0.679(44)
3.0	-0.245(16)	-0.093(16)	4.923(72)	0.840(50)
2.5	-0.616(29)	-0.045(14)	5.105(89)	1.154(66)
2.0	-1.180(68)	-0.027(21)	5.13(14)	1.087(81)
1.5	-2.26(17)	-0.061(56)	5.61(25)	0.988(75)

$\gamma$  of this model which were not observed in our previously published study [7]. Additionally, we provided improved estimates of the critical exponent  $\nu$ , the confluent correction exponent  $\omega$ , and updated the estimated critical temperatures for various correlation exponents  $a$  and concentrations of defects  $p_d$ . All directly measured critical exponents as well as critical exponents calculated through scaling relations are summarized in Table VI.

The obtained critical temperatures agree with those estimated by other groups for the uncorrelated disorder case. However, the temperatures for the correlated disorder cases are not compatible with other works. We expect that the

critical temperatures depend not only on the  $a$  and  $p_d$  parameters but also on the subtle details of the disorder generation process.

The main qualitative outcome of the study is the verification of the conjecture by Weinrib and Halperin [18], Eqs. (1) to (4), as the leading behavior for the long-range correlated disorder case with  $a \leq 3.0 = d$ . Our results suggest that additional terms need to be considered to improve the estimated behavior of the critical exponents given in Eqs. (1)–(4). We do not agree on the results from Refs. [24,25] which suggest a behavior very different from Eqs. (1)–(4).

For the uncorrelated case with  $a = \infty$ , we agree with the results observed by other groups to a great extent. An exception is the exponent  $\beta$  and the reason for this discrepancy remains unclear to us. Further, we see a possible violation of the hyperscaling relation in the crossover region around  $a \approx 3.0$ . Such a crossover effect would not be surprising, but to be evident, further analyses of this region are needed. One important problem at this point is that the correlation function between the defects decays very fast in this region and hence in principle, larger lattice sizes are needed to provide sufficient statistics.

## ACKNOWLEDGMENTS

The authors thank the Max Planck Society, IMPRS-MIS and especially the Max Planck Institute for Mathematics in the Sciences for financial support of this paper and for providing the computational resources at Max Planck Computing and Data Facility. They also gratefully acknowledge further support by the Deutsch-Französische Hochschule (DFH-UFA) through the Doctoral College  $\mathbb{L}^4$  under Grant No. CDFa-02-07. Many thanks go to Christophe Chatelain, Malte Henkel, and Mikhail Nalimov for discussions and deeper insights into the topic.

- [1] A. B. Harris, Effect of random defects on the critical behaviour of Ising models, *J. Phys. C: Solid State Phys.* **7**, 1671 (1974).
- [2] H. G. Ballesteros, L. A. Fernández, V. Martín-Mayor, A. Muñoz Sudupe, G. Parisi, and J. J. Ruiz-Lorenzo, Critical exponents of the three-dimensional diluted Ising model, *Phys. Rev. B* **58**, 2740 (1998).
- [3] P. Calabrese, V. Martín-Mayor, A. Pelissetto, and E. Vicari, Three-dimensional randomly dilute Ising model: Monte Carlo results, *Phys. Rev. E* **68**, 036136 (2003).
- [4] P. E. Berche, C. Chatelain, B. Berche, and W. Janke, Bond dilution in the 3D Ising model: A Monte Carlo study, *Eur. Phys. J. B* **38**, 463 (2004).
- [5] A. K. Murtazaev, I. K. Kamilov, and A. B. Babaev, Critical behavior of a cubic-lattice 3D Ising model for systems with quenched disorder, *J. Exp. Theor. Phys.* **99**, 1201 (2004).
- [6] M. Hasenbusch, F. P. Toldin, A. Pelissetto, and E. Vicari, The universality class of 3D site-diluted and bond-diluted Ising systems, *J. Stat. Mech.* (2007) P02016.
- [7] S. Kazmin and W. Janke, Critical exponent  $\nu$  of the Ising model in three dimensions with long-range correlated site disorder analyzed with Monte Carlo techniques, *Phys. Rev. B* **102**, 174206 (2020).
- [8] D. V. Pakhnin and A. I. Sokolov, Five-loop renormalization-group expansions for the three-dimensional  $n$ -vector cubic model and critical exponents for impure Ising systems, *Phys. Rev. B* **61**, 15130 (2000).
- [9] R. Folk, Y. Holovatch, and T. Yavors’kii, Effective and asymptotic critical exponents of a weakly diluted quenched Ising model: Three-dimensional approach versus  $\sqrt{\epsilon}$  expansion, *Phys. Rev. B* **61**, 15114 (2000).
- [10] A. Pelissetto and E. Vicari, Randomly dilute spin models: A six-loop field-theoretic study, *Phys. Rev. B* **62**, 6393 (2000).
- [11] M. V. Kompaniets, A. Kudlis, and A. I. Sokolov, Critical behavior of the weakly disordered Ising model: Six-loop  $\sqrt{\epsilon}$  expansion study, *Phys. Rev. E* **103**, 022134 (2021).
- [12] R. J. Birgeneau, R. A. Cowley, G. Shirane, H. Yoshizawa, D. P. Belanger, A. R. King, and V. Jaccarino, Critical behavior of a site-diluted three-dimensional Ising magnet, *Phys. Rev. B* **27**, 6747 (1983).
- [13] D. Belanger, J. Wang, Z. Slanič, S.-J. Han, R. Nicklow, M. Lui, C. Ramos, and D. Lederman, Neutron scattering study of the random field Ising film  $\text{Fe}_{0.5}\text{Zn}_{0.5}\text{F}_2$ , *J. Magn. Magn. Mater.* **140-144**, 1549 (1995).

- [14] P. W. Mitchell, R. A. Cowley, H. Yoshizawa, P. Boni, Y. J. Uemura, and R. J. Birgeneau, Critical behavior of the three-dimensional site-random Ising magnet:  $\text{Mn}_x\text{Zn}_{1-x}\text{F}_2$ , *Phys. Rev. B* **34**, 4719 (1986).
- [15] Z. Slanič and D. P. Belanger, The random-field specific heat critical behavior at high magnetic concentration:  $\text{Fe}_{0.93}\text{Zn}_{0.07}\text{F}_2$ , *J. Magn. Magn. Mater.* **186**, 65 (1998).
- [16] Z. Slanič, D. Belanger, and J. Fernandez-Baca, Random-field critical scattering at high-magnetic concentration in the Ising antiferromagnet  $\text{Fe}_{0.93}\text{Zn}_{0.07}\text{F}_2$ , *J. Magn. Magn. Mater.* **177-181**, 171 (1998).
- [17] R. Folk, Y. Holovatch, and T. Yavorskii, Critical exponents of a three-dimensional weakly diluted quenched Ising model, *Phys. Usp.* **46**, 169 (2003).
- [18] A. Weinrib and B. I. Halperin, Critical phenomena in systems with long-range correlated quenched disorder, *Phys. Rev. B* **27**, 413 (1983).
- [19] J. Honkonen and M. Y. Nalimov, Crossover between field theories with short-range and long-range exchange or correlations, *J. Phys. A: Math. Gen.* **22**, 751 (1989).
- [20] A. L. Korzhenevskii, A. A. Luzhkov, and W. Schirmacher, Critical behavior of crystals with long-range correlations caused by point defects with degenerate internal degrees of freedom, *Phys. Rev. B* **50**, 3661 (1994).
- [21] A. L. Korzhenevskii, A. A. Luzhkov, and H.-O. Heuer, Critical behaviour of systems with long-range correlated quenched defects, *Europhys. Lett.* **32**, 19 (1995).
- [22] H. G. Ballesteros and G. Parisi, Site-diluted three-dimensional Ising model with long-range correlated disorder, *Phys. Rev. B* **60**, 12912 (1999).
- [23] D. Ivaneyko, B. Berche, Y. Holovatch, and J. Ilnytskyi, On the universality class of the 3d Ising model with long-range correlated disorder, *Physica A* **387**, 4497 (2008).
- [24] V. V. Prudnikov, P. V. Prudnikov, and A. A. Fedorenko, Field-theory approach to critical behavior of systems with long-range correlated defects, *Phys. Rev. B* **62**, 8777 (2000).
- [25] V. V. Prudnikov, P. V. Prudnikov, S. V. Dorofeev, and V. Y. Kolesnikov, Monte Carlo studies of critical behaviour of systems with long-range correlated disorder, *Condens. Matter Phys.* **8**, 213 (2005).
- [26] N. G. Fytas and P. E. Theodorakis, Universality in disordered systems: The case of the three-dimensional random-bond Ising model, *Phys. Rev. E* **82**, 062101 (2010).
- [27] P. E. Theodorakis and N. G. Fytas, Wang-Landau study of the 3D Ising model with bond disorder, *Eur. Phys. J. B* **81**, 245 (2011).
- [28] W. Wang, H. Meier, J. Lidmar, and M. Wallin, Three-dimensional universality class of the Ising model with power-law correlated critical disorder, *Phys. Rev. B* **100**, 144204 (2019).
- [29] H. G. Ballesteros, L. A. Fernández, V. Martín-Mayor, A. M. Sudupe, G. Parisi, and J. J. Ruiz-Lorenzo, Ising exponents in the two-dimensional site-diluted Ising model, *J. Phys. A: Math. Gen.* **30**, 8379 (1997).
- [30] V. S. Dotsenko and V. S. Dotsenko, Critical behaviour of the phase transition in the 2D Ising model with impurities, *Adv. Phys.* **32**, 129 (1983).
- [31] J.-K. Kim and A. Patrascioiu, Critical behavior of the two-dimensional site-diluted Ising system, *Phys. Rev. B* **49**, 15764 (1994).
- [32] R. Kenna and J. J. Ruiz-Lorenzo, Scaling analysis of the site-diluted Ising model in two dimensions, *Phys. Rev. E* **78**, 031134 (2008).
- [33] G. Mazzeo and R. Kühn, Critical behavior of the two-dimensional spin-diluted Ising model via the equilibrium ensemble approach, *Phys. Rev. E* **60**, 3823 (1999).
- [34] P. H. L. Martins and J. A. Plascak, Universality class of the two-dimensional site-diluted Ising model, *Phys. Rev. E* **76**, 012102 (2007).
- [35] J. J. Ruiz-Lorenzo, Griffiths singularities in the two-dimensional diluted Ising model, *J. Phys. A: Math. Gen.* **30**, 485 (1997).
- [36] L. F. da Silva, U. L. Fulco, and F. D. Nobre, The two-dimensional site-diluted Ising model: A short-time-dynamics approach, *J. Phys.: Condens. Matter* **21**, 346005 (2009).
- [37] R. Shankar, Exact Critical Behavior of a Random Bond Two-Dimensional Ising Model, *Phys. Rev. Lett.* **58**, 2466 (1987).
- [38] B. N. Shalaev, Critical behavior of the two-dimensional Ising model with random bonds, *Phys. Rep.* **237**, 129 (1994).
- [39] A. Roder, J. Adler, and W. Janke, High-Temperature Series Analysis of 2D Random-Bond Ising Ferromagnets, *Phys. Rev. Lett.* **80**, 4697 (1998).
- [40] A. Roder, J. Adler, and W. Janke, High-temperature series analysis of the free energy and susceptibility of the 2D random-bond Ising model, *Physica A* **265**, 28 (1999).
- [41] C. Chatelain, Griffiths phase and critical behavior of the two-dimensional Potts models with long-range correlated disorder, *Phys. Rev. E* **89**, 032105 (2014).
- [42] C. Chatelain, Infinite disorder and correlation fixed point in the Ising model with correlated disorder, *Eur. Phys. J.: Spec. Top.* **226**, 805 (2017).
- [43] The exponents  $\nu$  and  $\eta$  are taken from F. Kos, D. Poland, D. Simmons-Duffin, and A. Vichi, Precision islands in the Ising and  $O(N)$  models, *J. High Energy Phys.* **08** (2016) 036; The correction exponent  $\omega$  is taken from D. Simmons-Duffin, The lightcone bootstrap and the spectrum of the 3d Ising CFT, *ibid.* **03** (2017) 086 [for an earlier estimate see also S. El-Showk, M. F. Paulos, D. Poland, S. Rychkov, D. Simmons-Duffin, and A. Vichi, Solving the 3d Ising model with the conformal bootstrap II.  $c$ -minimization and precise critical exponents, *J. Stat. Phys.* **157**, 869 (2014)].
- [44] A. M. Ferrenberg, J. Xu, and D. P. Landau, Pushing the limits of Monte Carlo simulations for the three-dimensional Ising model, *Phys. Rev. E* **97**, 043301 (2018).
- [45] D. P. Landau and K. Binder, *A Guide to Monte Carlo Simulations in Statistical Physics*, 3rd ed. (Cambridge University Press, New York, 2009)
- [46] M. E. J. Newman and G. T. Barkema, *Monte Carlo Methods in Statistical Physics* (Oxford University Press Inc., New York, 1999).
- [47] J. Zierenberg, N. Fricke, M. Marenz, F. P. Spitzner, V. Blavatska, and W. Janke, Percolation thresholds and fractal dimensions for square and cubic lattices with long-range correlated defects, *Phys. Rev. E* **96**, 062125 (2017).
- [48] H. Makse, S. Havlin, H. E. Stanley, and M. Schwartz, Novel method for generating long-range correlations, *Chaos, Solitons & Fractals* **6**, 295 (1995).
- [49] R. H. Swendsen and J.-S. Wang, Nonuniversal Critical Dynamics in Monte Carlo Simulations, *Phys. Rev. Lett.* **58**, 86 (1987).

- [50] W. Janke, Monte Carlo simulations in statistical physics – From basic principles to advanced applications, in *Order, Disorder and Criticality: Advanced Problems of Phase Transition Theory*, edited by Y. Holovatch (World Scientific, Singapore, 2012), Vol. 3.
- [51] A. M. Ferrenberg and R. H. Swendsen, New Monte Carlo Technique for Studying Phase Transitions, *Phys. Rev. Lett.* **61**, 2635 (1988).
- [52] J. Shao and D. Tu, *The Jackknife and Bootstrap*, Springer Series in Statistics (Springer, New York, 1995).
- [53] B. Efron and R. Tibshirani, *An Introduction to the Bootstrap*, Monographs on Statistics and Applied Probability (Chapman & Hall, New York, 1993), Vol. 57.
- [54] V. Blavats'ka, C. von Ferber, and Y. Holovatch, Polymers in long-range-correlated disorder, *Phys. Rev. E* **64**, 041102 (2001).
- [55] H.-O. Heuer, Critical crossover phenomena in disordered Ising systems, *J. Phys. A: Math. Gen.* **26**, L333 (1993).
- [56] S. Wiseman and E. Domany, Self-averaging, distribution of pseudocritical temperatures, and finite size scaling in critical disordered systems, *Phys. Rev. E* **58**, 2938 (1998).
- [57] J. Adler, Y. Meir, A. Aharony, and A. B. Harris, Series study of percolation moments in general dimension, *Phys. Rev. B* **41**, 9183 (1990).
- [58] N. Jan and D. Stauffer, Random site percolation in three dimensions, *Int. J. Mod. Phys. C* **09**, 341 (1998).
- [59] R. Badke, P. Reinicke, and V. Rittenberg, The discrete cubic and chiral cubic spin systems in various dimensions and their large- $n$  limits, *J. Phys. A: Math. Gen.* **18**, 653 (1985).
- [60] W. Janke, Monte Carlo methods in classical statistical physics, in *Computational Many-Particle Physics*, Lecture Notes in Physics No. 739, edited by H. Fehske, R. Schneider, and A. Weiße (Springer, Berlin, Heidelberg, 2008), pp. 79–140.
- [61] B. D. Josephson, Inequality for the specific heat: I. Derivation, *Proc. Phys. Soc.* **92**, 269 (1967).
- [62] B. D. Josephson, Inequality for the specific heat: II. Application to critical phenomena, *Proc. Phys. Soc.* **92**, 276 (1967).
- [63] G. S. Rushbrooke, On the thermodynamics of the critical region for the Ising problem, *J. Chem. Phys.* **39**, 842 (1963).